Measurement 94 (2016) 265–272

Contents lists available at ScienceDirect

Measurement

journal homepage: www.elsevier.com/locate/measurement

Development of a strain measurement system for the study of effect of relative humidity on wood

Kunjalata Kalita *, Nipan Das, Pradip Kumar Boruah, Utpal Sarma

Dept. of Instrumentation & USIC, Gauhati University, Assam 781014, India

ARTICLE INFO

Article history:
Received 10 September 2015
Received in revised form 30 July 2016
Accepted 1 August 2016
Available online 6 August 2016

Keywords:
Relative humidity
Signal conditioning circuit
Dimensional change of wood
Calibration

ABSTRACT

Wood is a widely used material in various applications where its dimensional stability is of practical interest in the design and performance of wooden materials. The change in geometry of wood depends upon the environmental conditions (such as relative humidity) as well as internal structure and composition of wood. This work presents a measurement technique and development of the associated system for the measurement of strain changes of wood samples with relative humidity. The developed system is capable of measuring the strain change and relative humidity (RH) with temperature compensation. The system comprises of strain gauge based strain measurement unit and RH sensor with its related signal conditioning circuit along with temperature sensor. The strain gauge signal conditioning is based on quarter bridge method with high precision resistors which is excited by an AC source. The whole system is centered on an 8-bit RISC microcontroller (PIC18F43K22). The built in 10-bit analog to digital converter (ADC) is used to read the strain and ambient RH. The temperature is directly read from temperature to digital converter using ZACwire™ interface. The measurement system is calibrated using a cantilever of stainless steel and is used for collecting and analyzing data of four wood samples. The uncertainties associated with the measurements are reported in the paper. Experimental results obtained for a few wood samples are presented.

1. Introduction

Humidity affects many properties of air, and of materials in contact with air. Water vapour is a key agent in both weather and climate, and it is an important atmospheric greenhouse gas. A huge variety of manufacturing, storage and testing process are humidity-critical. Humidity measurements are used wherever there is a need to prevent condensation, corrosion, mould, warping or other spoilage of products. This is highly relevant for foods, pharmaceuticals, chemicals, fuels, wood, paper, and many other products [1]. Measurement of relative humidity (water vapour present in air) is also essential for different scientific research and various situations where monitoring and control of environment is necessary. The effect of humidity is of paramount importance in wide range of application areas, such as moisture sensitive manufactured goods, textile, food processing, metrology, clinical instrumentation, integrated chips production, study of the growth of micro organism in living environment [2–4]. Baker et al. reported the effect of RH on the biocontaminant microenvironment have a spatial scale of the order of few millimeter [5]. Wood is a natural composite material with a hierarchical architecture which exhibits complex anisotropic mechanical and swelling behavior. As a hygroscopic material, wood responds to changes in environmental humidity by changing its geometry. Dimensional stability of wooden materials is of practical interest in the design of durable buildings and structures [6]. Wood exchanges moisture with air, the amount and direction of the exchange (gain or loss) depend on the relative humidity and temperature of the air and the current amount of water in the wood. Wood is anisotropic with regard to shrinkage and swelling. The magnitude of shrinkage and swelling is affected by the amount of moisture, which is lost or gained by wood [7]. Several endeavours have been practised and are still going on to study wood behavior with the changes of environmental humidity. Dominique Derome et al. studied the hysteretic swelling and shrinkage for latewood and earlywood by phase contrast X-ray tomography [8]. Ahmed et al. analyzed the estimation of the free swelling behavior of Norway spruce softwood. In this work, they predict the transverse anisotropy in the swelling behavior of softwood on the basis of periodic honeycomb unit cell model [6]. Steffen et al. determined the elastic modulus of wood cell wall material using a new in situ testing technique. This new technique

* Corresponding author.
E-mail address: kunjalatakalita@yahoo.co.in (K. Kalita).

http://dx.doi.org/10.1016/j.measurement.2016.08.001
0263-2241/

depends on a focused ion beam system (FIB) to prepare samples. Cantilevers are cut with the FIB from wood cell and loaded with a known force [9]. Ahmad et al. documented the hygroscopic swelling and shrinkage of the central and the thickest secondary cell wall layer of wood in response to changes in environmental humidity using synchrotron radiation-based phase contrast X-ray tomographic nanoscopy. They found that the volumetric strains at the cell wall level are significantly larger than those observed at cellular tissue [10]. Hassel et al. studied the performance of a wooden block shear wall which utilizes compressed wood as a connecting element in place of the traditional metal connectors [11].

To use wood to its best advantage and most effectively in engineering applications specific characteristics or physical properties must be considered. The versatility of wood is demonstrated by a wide variety of products. This variety is a result of a spectrum of desirable physical characteristics among many species of wood [7]. Laghdir et al. developed a technique for measuring the engineering coefficients of the 3D elasticity tensor of wood. In this method semi ring extensometer is used to study the coefficients [12]. The main drawback of this technique is the screw hole effect and temperature drift while taking both the axial and transverse strain measurement simultaneously on the same specimen. In order to characterize the mechanical properties, knowledge of the stress–strain relationships in the different directions is required. For that purpose Dahl et al. developed video extensometer technique for the measurement of planer strain of wood [13]. The use of an optical measurement system applied to the mechanical characterization of thin microtome sections of spruce is reported by Sinn [14]. They presented an optical measurement system for the determination of strains and displacements of wood specimens [14].

To study the change in strain of wood with RH it is essential to have a precise measurement system for measuring both change in RH and corresponding changes in strain of the sample. Proper signal conditioning circuits are employed to increase the reliability of the developed system. In this work, strain gauges are used to measure the strain developed on the surface of wood samples due to change in RH. The developed strain measurement system is calibrated by a simple and convenient cantilever beam method using different loads. The present measurement system is capable of measuring and monitoring the RH, temperature and strain of wood samples. To measure RH and strain of wood samples analog sensors are used where as a digital sensor is used to measure temperature. The analog and digital sensors are sequentially read by PIC18F43K22 microcontroller. The system firmware for microcontroller is developed on MPLAB-IDE and suitable codes are written on C-language for handling data in the PC side.

To study the effect of RH in wood samples, different levels of RH are necessary for the experiment. There are four-types of standard humidity generator systems: (1) two-pressure humidity generator [15], (2) two temperature humidity generator [16], (3) divided-flow humidity generator, and [15,17] (4) fixed-point humidity systems [17,18]. Except for the fixed-point humidity systems, others can provide more accurate standard environment [15]. However, they are expensive and complicated. Sometime, an experimental factory setup is required to install these systems, whereas, certified fixed RH points with saturated salt solutions are easier to setup. This fixed point method is inexpensive, convenient, and easy to be reproduced in a research laboratory. It is often used as check points for humidity sensors. However, the fixed values of RH limit the applicable range of this type of setup and accuracy depends on the purity of the salts used [15]. To test the variation of strain of different wood samples with RH, four different binary saturated salt solutions are used to generate different level of humidity within desiccators. The RH and temperature inside the desiccator are continuously monitored until they reach stable level of humidity. Strain developed in the wood samples is measured when RH attains stable level.

2. System architecture

The basic block diagram of the measurement system is shown in Fig. 1.

The system is designed incorporating TSIC 506F temperature sensor, HIH5030 humidity sensor and CF350-2AA (11) C20 strain gauge which are interfaced to PIC18F43K22 microcontroller and connected to PC by RS232 communication. The outputs of humidity sensor HIH5030 and four strain gauges (CF350-2AA (11) C20) are fed to the five channels of the on-chip 10-bit ADC of the PIC18F43K22 microcontroller through signal conditioning circuit. The temperature sensor TSIC 506F is interfaced to the microcontroller by ZACwire™ [18]. A 20×4 LCD serve as a local display and RS 232 communication is employed to provide the facility for data logging. The system software for microcontroller is developed on MPLAB-IDE and suitable codes are written in C-language for handling data in the PC side.

3. Implementation

For implementing the system different modules are developed separately and finally integrated together for proper functionality. Signal conditioning circuits are designed to get voltage output in the input range of the integrated ADC of the microcontroller for the entire dynamic range of the sensors. Proper algorithm is developed to read the sensors and to get desired measurements of strain developed in wood samples along with temperature compensation for RH measurement. The developed code is implemented on the microcontroller. The measured values are displayed locally on 20×4 LCD and transmitted via RS232 communication to PC.

3.1. Sensors

For the measurement of temperature, low power TSIC 506F is used which provides digital output and accuracy of ±0.1 K combined with long term stability. The ZACwire™ interface compatible sensor TSIC which is a factory calibrated temperature sensor and the digital output (T) of the sensor is given by [18]

$$T = \left[\frac{D}{2047} \times (T_H - T_L) + T_L\right] \tag{1}$$

where D is the 8 bit data from the temperature sensor and $(T_H - T_L)$ being the temperature range of the sensor with $T_L = -10\,^{\circ}\mathrm{C}$ and $T_H = 60\,^{\circ}\mathrm{C}$.

HIH5030 is used for the measurement of relative humidity. The HIH-5030 series low voltage humidity sensors operate down to 2.7 V_{dc}. The accuracy of the humidity sensor is ±3%. The output voltage V_{out} and RH is related by the following equation at 25 °C [19]

The output voltage V_{out} and RH of the humidity sensor HIH-5030 are related by the following equation at 25 °C [19]

$$\mathrm{RH} = \left[\frac{V_{out}}{0.00636 \times V_{supply}} - 23.82\right]\% \tag{2}$$

Temperature compensated $(\mathrm{RH})_T$ and is given by the following equation [19]

$$(\mathrm{RH})_T = \left[\frac{\mathrm{RH}}{(1.0546 - 0.00216T)}\right]\% \tag{3}$$

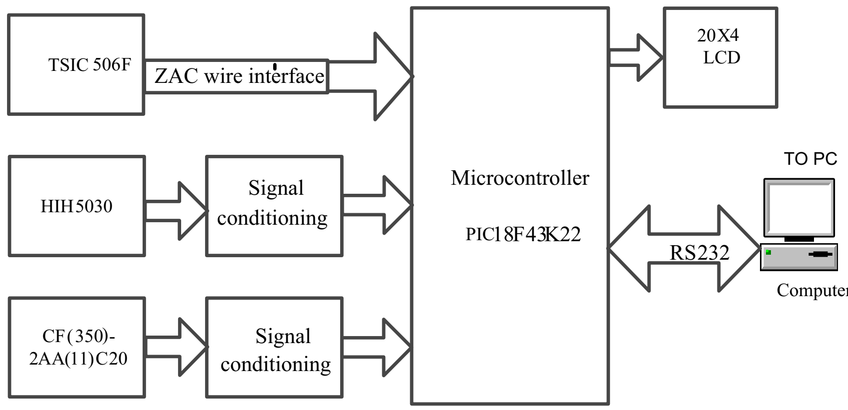

Fig. 1. Block diagram of the measurement system.

The Humidity sensor and temperature sensor are assembled close to each other to minimize the temperature gradient between them.

For measuring the strain of wood sample CF350-2AA (11) C20 strain gauge sensor is used which has the nominal resistance 350 Ω with gauge factor 2.13 ± 1%.

3.2. Signal conditioning for strain gauge

A block diagram of the signal conditioning for strain gauge is shown in Fig. 2.

A quarter bridges with three fixed resistors and one strain gauge (which is attached to the wood sample) is used for strain measurement. Each of the 350 Ω fixed value resistors has tolerance of ±0.1% and temperature co-efficient ±5 ppm/°C which ensure very low temperature drift. The bridge is excited by 1 kHz, 5 V (peak-peak) sinusoidal signal (amplitude accuracy, ±1 mV peak to peak) from the Agilent Function generator (Model no. 33220A). The differential output of the bridge is amplified by an instrumentation amplifier (AD620) and the amplified AC output is converted to DC by using peak detector (Fig. 3).

The transfer function of the signal conditioning circuit (Fig. 3) is given by

$$\frac{V_{out}}{strain} = \left(\frac{49.4\ \text{K}\Omega}{Rg} + 1\right) \times \frac{V_{in}}{8} \times \frac{\Delta R}{R} \quad (4)$$

where V_{in} the excitation voltage, ΔR the change in resistance of the sensor and R is the resistance of the sensor in the unstrained condition, R_g is the gain setting resistor.

3.3. Interface

Interface of the sensor and signal conditioner with the microcontroller is done with the on-chip 10-bit A/D converter. The reference voltage is generated internally and is configured at 4.096V. The functioning of the A/D converter is controlled by PIC 18F43K22 (Microchip). For PC interface via RS232, MAX232 is used as level shifter and the communication is done at 9600 baud rate, 8 data bits, 1 stop bit and no parity bit.

3.4. Algorithm of the firmware

The necessary algorithm for the system is implemented on PIC 18F43K22 microcontroller using MPLAB-IDE. The algorithm is as follows:

(i) Initialize A/D converter, LCD, UART (Universal Asynchronous Receiver Transmitter).
(ii) Read A/D converter for different samples of wood, RH sensor and temperature sensor.
(iii) Calculate true RH using Eq. (3) for temperature compensation
(iv) The compensated RH, temperature value and strain of the samples in terms of mV is displayed on the LCD and send to the PC in ASCII format by RS232 communication.

To manage the received data a suitable code is written in C language. It receives the ASCII data from the system and displays time, temperature, RH, strain in mV of the sample. Data are stored in PC in .XLS format along with records of time.

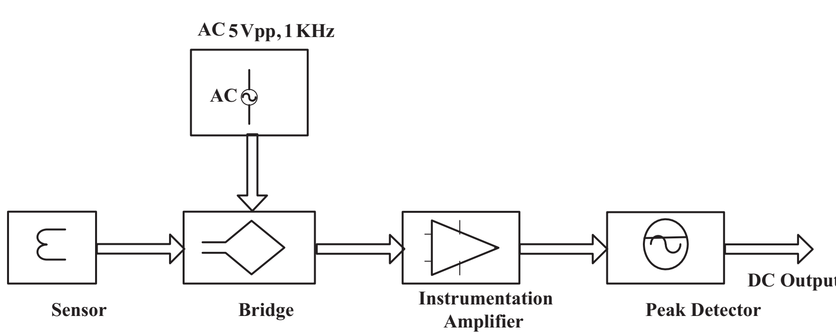

Fig. 2. Block diagram of the signal conditioning circuit of the strain gauge.

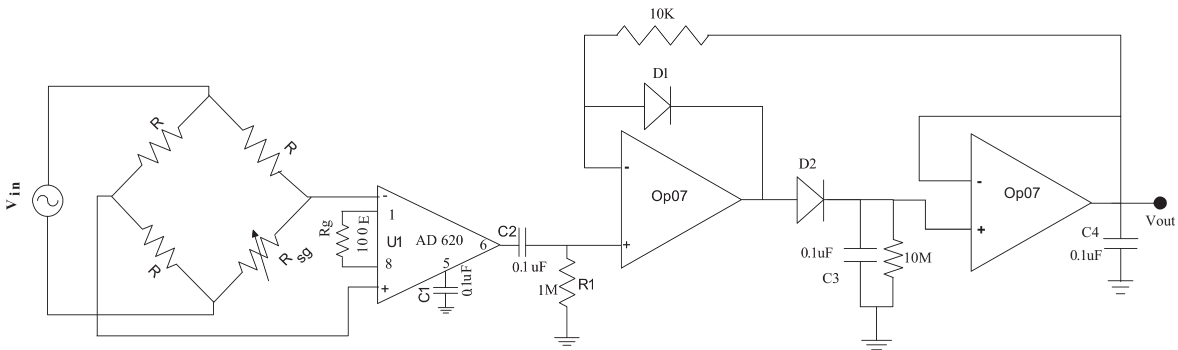

Fig. 3. Signal conditioning circuit of the strain gauge.

4. Experimental methods and findings

4.1. Calibration

A rectangular beam of stainless steel is used to make a cantilever. The beam is fixed at one end and loaded at the other end using knife edge to remove shearing effect due to loading (see Fig. 4). The mass of the loads are measured by a balance (model no: AB54, make: Metler Toledo, sensitivity of 0.1 mg) prior to the experiment. Three strain gauges are attached to the surface of the beam with adhesive (cyanoacrylate) to measure tensile strain. Strain gauge is attached at the principal axis (geometrically measured at the half of the width) of the beam. Before attaching the strain gauges, the surface of the beam is cleaned and polished. The tensile strain (ε) for a cantilever is given by [20].

$$\varepsilon = \frac{6\,\text{mg}X}{bh^2E} \tag{5}$$

where m is the mass of the load, g is the acceleration due to gravity (9.78049 m/s^2), X is the distance from the strain gauge to load (0.2 m), b (0.0184 m), h (1.54×10^{-3} m), are the width and thickness of the cantilever beam respectively and the Young's modulus E (180×10^9 N m^{-2}) of the beam is measured by Instron-Dynamic UTM (Model: 8801J4051).

The error in the measurement of tensile strain involves contribution from the measurements of the following factors m, X, b and h. The instrumental error in measuring m is $\delta m = 1 \times 10^{-7}$ kg, $\delta X = \delta b = \delta h = 1 \times 10^{-6}$ m. Hence, the total fractional error is calculated as

$$\frac{\delta(\varepsilon)}{\varepsilon} = \sqrt{\frac{\delta_m^2}{m^2} + \delta_x^2\left[\frac{1}{X^2} + \frac{1}{b^2} + \frac{4}{h^2}\right]} = 1.3 \times 10^{-3} \tag{6}$$

Using least square regression method, the calculated strain and output voltages for different loads are plotted shown in Fig. 5.

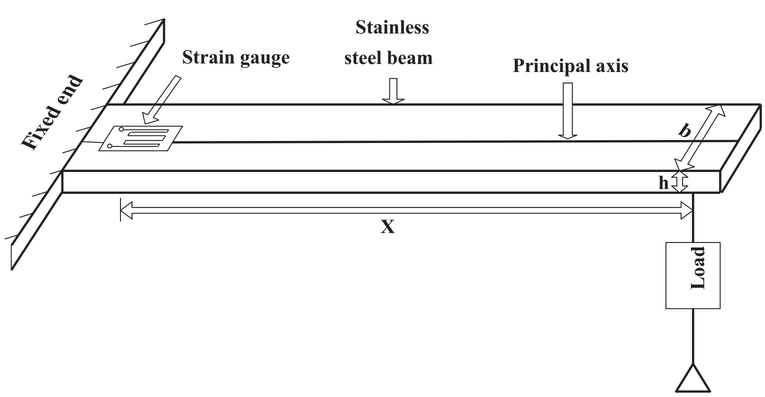

Fig. 4. Calibration setup.

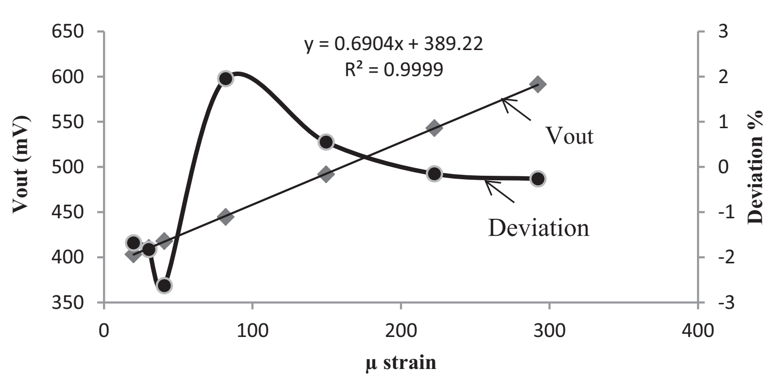

Fig. 5. Calibration curve and deviation of the measured voltage from the expected value.

The calibration curve is given as

$$y = 0.69x + 389.2 \quad (7)$$

where y represents the output voltage in mV and x is the μstrain (με).

The slope of the fitted curve gives a measure of the sensitivity of the system as 0.69 mV/με. The deviation of the measured voltage from the expected value is shown in Fig. 5. The maximum deviation is 2.6%.

4.2. Validation of calibration equation

For validation of the calibration equation the output voltage in mV is measured for different loads for the stainless steel used for calibration and a copper cantilever. The corresponding microstrains are calculated using Eq. (7). The values of E for both the material have been reproduced using Eq. (5). The values of E of the beams are also measured by Instron-Dynamic UTM (Model: 8801J4051) and the results are presented in Table 1.

Table 1
Young's modulus of different materials.

Material	Standard value of E (10^9 N/m^2)	Value of E measured by the system (10^9 N/m^2)	Relative error %	Value of E measured by Standard equipment (Instron-Dynamic UTM, 10^9 N/m^2)
Stainless steel	180	179 ± 2.8	0.56	180
Copper	117	116 ± 5.4	0.86	117

Table 2
Samples of pine and dimensions.

Samples	Dimension of the samples
S1	5 cm × 1.7 cm × 0.8 cm
S2	5 cm × 1.7 cm × 1.3 cm
S3	5 cm × 1.7 cm × 2.8 cm
S4	5 cm × 1.7 cm × 4.5 cm

Table 3
Levels of humidity generated by binary salt solutions at 25 °C.

Salt name	RH (%)	Absolute uncertainty in RH (%)
Lithium chloride	11.30	±0.27
Potassium acetate	22.51	±0.32
Magnesium chloride	32.78	±0.16
Magnesium nitrate	52.89	±0.22
Sodium chloride	75.29	±0.12

4.3. Testing of the system

4.3.1. Sample preparation and sensor attachment

Before attaching the strain gauges to the wood samples, the wood samples are prepared well to record strain change with minimum artifacts.

Four wood samples of pine (*Pinus* spp.) in different sizes are chosen and prepared for experiment. The wood samples are cleaned well and polished with emery paper of grit size 1500 to obtain a smooth surface. Prior to the experiments, the samples are oven dried at 90 °C and stored in a desiccator. 86.8% moisture content (determined by weight loss method) of the wood samples was lost due to oven drying.

Two strain gauges are attached by cyanoacrylate adhesive [21] on each of the sample, one in longitudinal and other in transverse direction. Finally the connecting leads are soldered and connected to the bridge circuits.

The wood samples and dimensions of the samples are given in Table 2.

4.3.2. Fixed point humidity generator and sample placement

Binary saturated salt solutions, prepared as per OIML R121 [15] in a desiccator at constant temperature generate fixed levels of humidity with uncertainties [14,15] as shown in Table 3. A desiccator sealed with silicon high vacuum grease is used in the experiment to generate different fixed levels of humidity using the salts shown in Table 3 [17]. The samples under test and sensors are placed inside the desiccator as shown in Fig. 6.

4.4. Experimental results

During the experiment the samples under test are placed inside the desiccator for different levels of humidity generated by various salt solutions at 25 °C (±1 °C). At the stable level of humidity, the mean of 1000 data recorded at an interval of one minute is considered. Variations of responses of the samples are observed for different levels of humidity and plotted in Figs. 7–10. The goodness of fit (R^2) values are mentioned on the curves (see Table 4).

The developed system is capable of detecting the strain over the surface due to change in ambient relative humidity. The strain change of wood samples is found to be linear with the change in RH. From the slopes of the linear regression fit it is observed that the strain sensitivity varies for different wood samples (for different thickness). The samples show different strain sensitivity

Fig. 6. Experimental setup during sample test at different RH level.

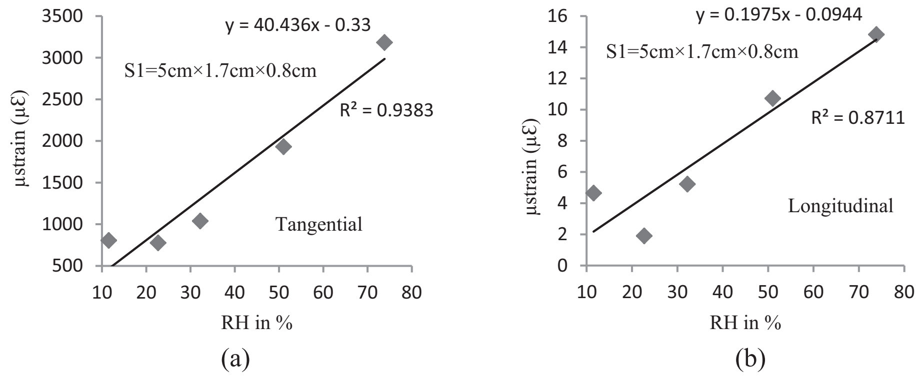

Fig. 7. Strain variation of S1 vs RH (a) in tangential and (b) longitudinal direction.

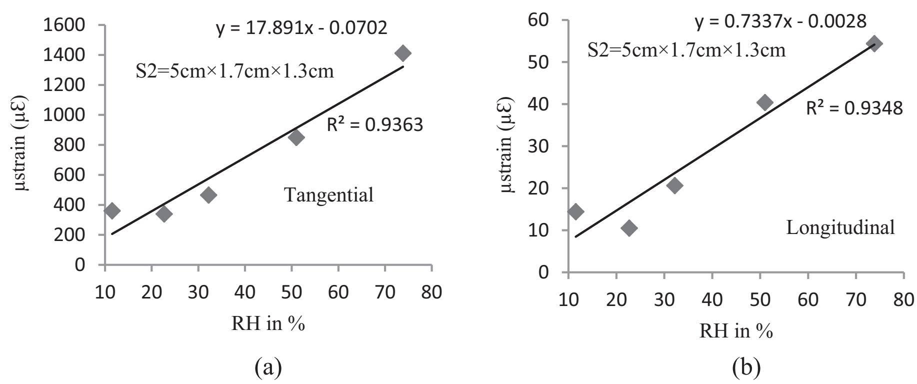

Fig. 8. Strain variation of S2 vs RH (a) in tangential and (b) longitudinal direction.

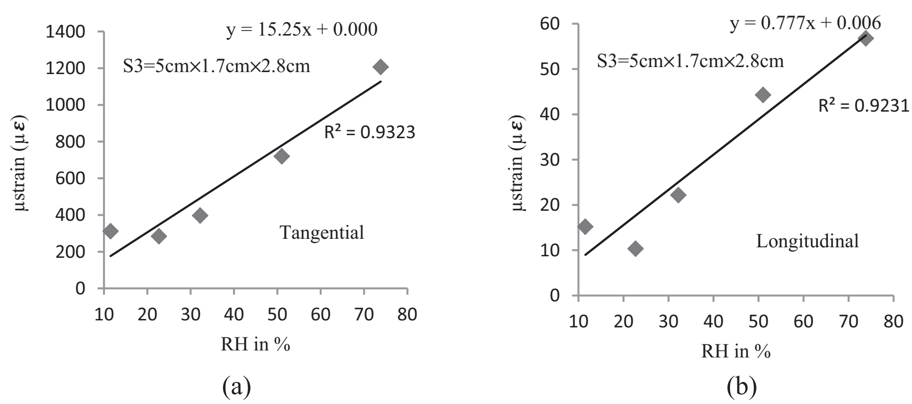

Fig. 9. Strain variation of S3 vs RH (a) in tangential and (b) longitudinal direction.

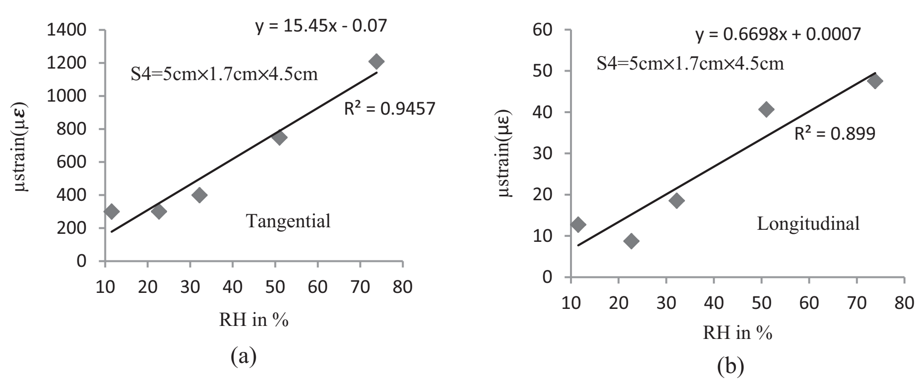

Fig. 10. Strain variation of S4 vs RH (a) in tangential and (b) longitudinal direction.

Table 4
Standard deviation of the samples at different humidity conditions.

RH (%)	Direction	Standard deviation (σ) in με			
		S1	S2	S3	S4
11.21	Longitudinal	1.46	1.79	1.62	1.79
	Tangential	1.46	1.49	1.47	1.42
22.10	Longitudinal	1.40	1.75	1.49	1.46
	Tangential	1.40	1.49	1.44	1.43
33.21	Longitudinal	1.50	2.91	0.98	1.50
	Tangential	1.42	1.75	0.25	1.72
52.01	Longitudinal	1.44	2.84	1.48	1.42
	Tangential	1.49	1.50	1.77	2.91
73.10	Longitudinal	1.50	1.46	0.24	1.62
	Tangential	1.50	1.53	1.46	3.07

in longitudinal and tangential direction. The strain sensitivities for S1, S2, S3 and S4 samples of pine in tangential and longitudinal directions are 40.43 με/RH, 0.197 με/RH, 17.89 με/RH, 0.733 με/RH, 15.25 με/RH, 0.777 με/RH, 15.45 με/RH, 0.699 με/RH respectively. It is also found that the thickness of the samples also affect the strain sensitivity.

4.5. Uncertainty evaluation of the system

For uncertainty analysis there are two approaches.

1. The Type A evaluation of standard uncertainty is the method of evaluation by the statistical analysis of observations [1].
2. The Type B evaluation of standard uncertainty is the method of evaluation by other information about the measurement [1].

The estimated standard uncertainty (u) can be calculated as [1]

$$u = \frac{\sigma}{\sqrt{n}} \tag{8}$$

where σ is standard deviation (SD), n is the number of measurements in a set.

In Table 5, Type A uncertainties are described. u_1, u_2, u_3, u_4, u_5 are the uncertainties of measurement at different humidity conditions.

Type B uncertainties are tabulated in Table 6.

4.5.1. Relative uncertainty of the system

From the transfer function Eq. (4), it is seen that the output voltage of the signal conditioning circuit depends on various factors, e.g. the supply voltage of the bridge, tolerance of the fixed resistors and strain gauge.

Table 6
Standard Type B uncertainty.

Error sources	Nominal values of the measurand	Maximum possible error value	Distribution type	Standard Type B uncertainty
V_{in}	5 V ± 1 mV	1 mV	Normal	1 mV
R_g	100 Ω ± 0.1%	1 Ω	Rectangular	$\frac{1\,\Omega}{\sqrt{3}} = 0.58\,\Omega$
ΔR	350 Ω ± 1%	3.5 Ω	Rectangular	$\frac{3.5\,\Omega}{\sqrt{3}} = 2.02\,\Omega$
R	350 Ω ± 0.1%	0.35 Ω	Rectangular	$\frac{0.35\,\Omega}{\sqrt{3}} = 0.20\,\Omega$

Excluding the constant terms (since they don't contribute uncertainty) relative uncertainty of the output, V_{out}, is calculated as below.

$$\frac{u(V_{out})}{V_{out}} = \sqrt{\left[\frac{u(R_g)}{R_g}\right]^2 + \left[\frac{u(V_{in})}{V_{in}}\right]^2 + \left[\frac{u(\Delta R)}{\Delta R}\right]^2 + \left[\frac{u(R)}{R}\right]^2}$$

where R_g is gain setting resistor with tolerance 0.1%, V_{in} is excitation voltage, ΔR is change in strain gauge's resistance with tolerance 1%, R is fixed resistor with tolerance 0.1%.

$$\frac{u(V_{out})}{V_{out}} = \sqrt{\left[\frac{0.1}{100}\right]^2 + \left[\frac{1}{5000}\right]^2 + \left[\frac{3.5}{350}\right]^2 + \left[\frac{.35}{350}\right]^2}$$

$$\frac{u(V_{out})}{V_{out}} = 1.10 \times 10^{-3}$$

5. Conclusion

A strain measurement system is successfully developed which can be used to study the effect of RH on wood. The advantage of the system is its capability of online data logging along with local monitoring. The sensitivity of the system in strain measurement is 0.69 mV/με with an accuracy of ±2.6%με. The temperature measurement has the resolution 0.034 °C with accuracy of 0.1 °C and the RH measurement has the accuracy of ±3%RH in the range of 0–100% RH.

Since the bridge is excited with AC voltage, the effects of $1/f$ noise and parasitic thermocouples are reduced. Also due to high common mode rejection ratio (100 dB) of the used instrumentation amplifier, electromagnetic interferences from line frequency (50 Hz) are minimized. Use of precision components in the bridge reduces the temperature drift. Temperature compensation in RH measurement is another advantage of the system.

The observations agree with the related literature i.e. the difference in sensitivities reveals that the strains are anisotropic within the same sample [7]. It is also found that the strain sensitivity is larger in the tangential direction than in the direction of longitudinal direction.

Table 5
Standard Type A uncertainty.

Type	Uncertainty in temperature at 25 °C	Uncertainty	RH (%)	Uncertainty in RH (%)	Uncertainty in μstrain (με)				
					Direction	S1	S2	S3	S4
Type A (using Eq. (8))	4.53×10^{-3}	u_1	11.21	2.87×10^{-3}	Longitudinal	0.046	0.057	0.051	0.057
					Tangential	0.046	0.047	0.046	0.045
		u_2	22.10	5.44×10^{-3}	Longitudinal	0.044	0.055	0.047	0.046
					Tangential	0.044	0.047	0.046	0.045
		u_3	33.21	3.82×10^{-3}	Longitudinal	0.047	0.092	0.031	0.047
					Tangential	0.045	0.055	0.008	0.054
		u_4	52.01	5.83×10^{-3}	Longitudinal	0.046	0.090	0.046	0.045
					Tangential	0.047	0.047	0.056	0.092
		u_5	73.10	6.98×10^{-3}	Longitudinal	0.047	0.046	0.008	0.051
					Tangential	0.047	0.048	0.046	0.097

Selection of proper wood based on dimensional stability for various engineering applications can be investigated using the developed system. The measurement system will also be used to study the shrinkage and swelling anisotropic behavior of wood in different humidity conditions. Further, it is proposed to use this system to study possibility of using wood samples as humidity sensors. It is also proposed to validate the effect of RH on deformation of wood samples due to ambient humidity by an independent method simultaneously with strain measurement method.

Acknowledgment

This study was supported in part by the Assam Science Technology and Environment Council (ASTEC), Assam under Grant ASTEC/S&T/1614(2)/2012/3215. Dr. Kalyanee Boruah, Prof. of Dept. of Physics, G.U. is acknowledged in supporting the preparation of the result. Shakeel Zamal is also acknowledged for his helpful suggestions during the work.

Appendix A. Supplementary material

Supplementary data associated with this article can be found, in the online version, at http://dx.doi.org/10.1016/j.measurement.2016.08.001.

References

[1] S. Bell, A Beginner's Guide to Humidity Measurement, National Physical Laboratory, 2011.
[2] R. Montanini, Wavelength-encoded optical psychrometer for relative humidity measurement, Rev. Sci. Instrum. 78 (2) (2007) 025103.
[3] T. Lu, C. Chen, Uncertainty evaluation of humidity sensors calibrated by saturated salt solutions, Measurement 40 (6) (2007) 591–599.
[4] U. Sarma, P.K. Boruah, Design and characterisation of a temperature compensated relative humidity measurement system with online data logging feature, Mapan 29 (2) (2014) 77–85.
[5] P.H. Baker, G.H. Galbraith, R.C. McLean, C.H. Sanders, The development of instrumentation for the measurement of relative humidity within building microenvironments, Measurement 39 (6) (2006) 565–574.
[6] A. Rafsanjani, C. Lanvermann, P. Niemz, J. Carmeliet, D. Derome, Multiscale analysis of free swelling of Norway spruce, Composites Part A 54 (2013) 70–78.
[7] GTR-FPL-I13, USDA Forest Service, Wood Handbook: Wood as an Engineering Material, Forest Product Laboratory, Madison, 1999.
[8] A. Rafsanjani, M. Stiefel, K. Jefimovs, R. Mokso, D. Derome, J. Carmeliet, Hygroscopic swelling and shrinkage of latewood cell wall micropillars reveal ultrastructural anisotropy, J. R. Soc. Interface 11 (2014) 95.
[9] S. Orso, G.K.U. Wegst, E. Arzt, The elastic modulus of spruce wood cell wall material measured by an in situ bending technique, J. Mater. Sci. 41 (2006) 5122–5126.
[10] D. Derome, A. Rafsanjani, A. Patera, R. Guyer, J. Carmeliet, Hygromorphic behavior of cellular material: hysterectic swelling and shrinkage of wood probed by phase contrast X-ray tomography, Phil. Mag. 92 (2012) 28–30.
[11] I. Hassel, P. Berard, K. Komatsu, Development of wooden block shear wall Improvement of stiffness by utilizing elements of densified wood, Holzforschung 62 (5) (2008) 584–590.
[12] A. Laghdir, Y. Fortin, C.M.D.L. Cruz, R.E. Hernandez, Development of technique to determine the 3d elasticity tensor of wood as applied to drying stress modeling, Maderas Ciencia y tecnología 10 (1) (2008) 35–44.
[13] K.B. Dahl, K.A. Malo, Planar strain measurements on wood specimens, Exp. Mech. 49 (2009) 575–586.
[14] G. Sinn, A. Reiterer, S.E. Stanzl-Tschegg, E.K. Tschegg, Determination of strains of thin wood samples using videoextensometry, vol. 59, Springer-verlag, 2001, pp. 177–182.
[15] P.R. Wiederhold, Water vapor Measurement: Methods and Instrumentation, CRC Press, 1997, pp. 121–124.
[16] P.G. Su, R.J. Wu, Uncertainty of humidity sensors testing by means of divided-flow generator, Measurement 36 (1) (2004) 21–27.
[17] L. Greenspam, Humidity fixed points of binary saturated aqueous solutions, J. Res. Natl. Bureau Stand 81 (A) (2004) 89–96.
[18] IST innovative sensor technology, Tsic 506F TO 92 (accessed on 2nd August, 2015).
[19] Honeywell, HIH-5030 (accessed on 1st August, 2015).
[20] J.M. Gere, Mechanics of Material, 6th ed., Bill Stenquist, 2004.
[21] Application note of Vishay precision group, <http://www.vishaypg.com/micro-measurements/installation-accessories/> (accessed on 12th March 2016).